

Polarization properties of light scattered by a metallic cylinder

G. López-Morales^{a,b,*}, I. Saucedo-Orozco^{a,b}, R. Espinosa-Luna^{a,b}, Q. Zhan^a, and F. Villa-Villa^b

^a*Department of Electro-Optics and Photonics, University of Dayton,
300 College Park, Dayton, Ohio 45469, USA*

^b*GIPYS, Centro de Investigaciones en Óptica, A. C.,
Loma del Bosque 115, Colonia Lomas del Campestre, 37150 León, Guanajuato, México.*

**e-mail: lopezmg@cio.mx*

Received 6 October 2016; accepted 2 May 2017

The experimental determination of the angularly resolved Mueller matrix associated to light scattered by a metallic cylinder is reported. The angle-dependent values of depolarization index and Gil-Bernabeu theorem confirm there are not depolarization effects. To our knowledge, this is the cheapest and easiest way to generate uniform linear horizontal and vertical polarizations scattered angularly. A possible application associated to the use of plastic optical fibers acting like a polarization de-multiplexer is briefly discussed.

Keywords: Polarization; Mueller matrix; analysis of polarized light.

Se reporta la determinación experimental de la matriz de Mueller resuelta angularmente, asociada a la luz esparcida por un cilindro metálico. Los valores angularmente dependientes del índice de despolarización y el teorema de Gil-Bernabeu confirman que los efectos de despolarización no se presentan. A nuestro entender, la configuración estudiada es la manera más barata y fácil de generar polarizaciones uniformes lineales horizontales y verticales esparcidas angularmente. Se menciona una posible aplicación asociada al uso de fibras ópticas de plástico, actuando como demultiplexores de polarización.

Descriptores: Polarización; matrices de Mueller; análisis de la luz polarizada.

PACS: 42.25.Ja

1. Introduction

A one-dimensional (1D) rough surface is a highly symmetric system, defined with respect to a Cartesian coordinate system as a surface whose profile (z -axis) varies only along the x -axis and is constant along the y -axis; for example, a diffraction grating. The scattering properties of 1D rough metallic and dielectric surfaces have been extensively reported theoretically, numerically and experimentally [1-10] and the polarimetric behavior has been reported using the Mueller-Stokes formalism [6-12].

On the other hand, a cylinder with axis oriented along the y -axis is also a highly symmetric system which can be considered as the minimum expression of what a 1D surface is build of, a single groove [13]. In this work, an experimental validation of this consideration will be proved through the determination of the polarimetric behavior for the scattering of light by metallic cylinders, when the illumination is perpendicular to the cylinder axis.

Due to its potential applications to many problems in radiative transfer, remote sensing, diagnosis, and particularly in forensic analysis of fibers, cylinders have been one of the main geometries studied [13-22]. Of particular importance has been the work done on the aspect ratio dependence of the light scattered by cylinders [13,14]. Some authors have applied simple models based on the geometrical theory of diffraction to obtain the diffraction pattern of the scattered light and then have calculated the cylinder diameter [21,22]. Experimental and theoretical studies related with the scattering of light by cylinders have been reported (optical fiber with

an evaporated thin film), where the elements of the Mueller matrix have been measured within an angular interval of 180° , but neither the polarization behavior as a function of the scattering angle nor their potential applications have been discussed [23-24]. In this work, an experimental validation of this consideration will be proved through the determination of the polarimetric behavior for the scattering of light by metallic cylinders, when the illumination is perpendicular to the cylinder axis. Recently, the scattering of light by cylinders under a conical geometry of incidence has given rise to a method to generate radial and azimuthal unconventional polarization states [25].

Here is reported the experimental determination of the 360° angularly scattered light by a metallic cylinder, where the results show the Mueller matrix obtained has the same form as the associated to a 1D surface, as expected. Even though both a partially reflecting 1D surface and a metallic cylinder can scatter any totally polarized incident light around 360° , under these circumstances the 1D surface depolarizes the incident polarization state (with the exception of the incident linear polarizations parallel and perpendicular to the generators or grooves of the surface) while the cylinder does not. Furthermore, from the MM parameters determined experimentally, scalar polarization metrics are calculated and applied in this work to prove the system studied here indeed does not depolarize the incident light at 632.8 nm. Due to the extensive theoretical and numerical work reported with the diffraction and scattering of light by metallic cylinders illuminated under both, plane and conical geometries of incidence, using linear polarizations parallel and

perpendicular to the cylinder axis, we will not repeat those results here. We suggest to the interested reader consult the Refs. [13-19,21-26].

2. Theory

The linear response to light can be determined through the Jones matrix, the coherence matrix or the Mueller matrix formalisms, depending on both the polarization of the incident light and the depolarization properties of the system under study [11,12]. It is interesting to take into account that the linear response depends also on the coherent properties of light, the incidence angle, and the own nature of the scattering sample under study.

The Mueller matrix (MM) is a 4×4 matrix whose elements are all real and represents the linear response to the incident intensity associated to the illuminating beam, whose polarization state is represented by a Stokes vector S (a 4×1 column matrix, with real elements).

$$S^{\text{out}} = MS^{\text{in}} \quad (1)$$

The form of the MM depends strongly on the morphological characteristics of the sample under study [20], but the Mueller parameter values depend on the nature of the sample. The MM parameters have also been determined, independently of the dielectric properties of the 1D surface and its depolarization properties, at the physical optics approximation limit [6-10,12]. A one-dimensional surface is associated to a Mueller matrix with the form given by Eq. (2) [6].

$$M_{1D} = \begin{bmatrix} m_{00} & m_{01} & 0 & 0 \\ m_{01} & m_{00} & 0 & 0 \\ 0 & 0 & m_{22} & m_{23} \\ 0 & 0 & -m_{23} & m_{22} \end{bmatrix} \quad (2)$$

Note that $m_{00} = m_{11}$, $m_{01} = m_{10}$, $m_{22} = m_{33}$, $m_{23} = -m_{32}$, and the elements m_{02} , m_{03} , m_{12} , m_{13} , m_{20} , m_{21} , m_{30} , m_{31} are zero. If the 1D surface does not depolarize the incident light, then only three parameters are independent, because $m_{00}^2 = m_{01}^2 + m_{22}^2 + m_{23}^2$. Eq. (2) is the polarimetric model that best describes the light scattered by the metallic cylinder illuminated perpendicularly to the cylinder axis [23,24]. The polarimetric parameters are relationships among the Mueller matrix elements used to describe some specific linear responses of the illuminated medium to the incident polarized intensity. The depolarization index, $DI(M)$, is defined as [27]

$$0 \leq DI(M) = \left\{ \sum_{j,k=0}^3 m_{jk}^2 - m_{00}^2 \right\}^{1/2} / \sqrt{3}m_{00} \leq 1 \quad (3)$$

It is interpreted as the depolarization average generated by the medium to the incident polarization. The depolarization index seems to depend only on the medium properties and not of the characteristics of the incident light. This is not really true, because the MM represents just the response to

the incident polarization. Its physical limits are interpreted as follows: 0 means the system depolarizes totally the incident light, while 1 means the system does not depolarize at all. The intermediate values are interpreted as a partial depolarization generated on the scattered light.

The theorem of Gil-Bernabeu or the trace condition, usually is employed to test if the system can be described by a Jones matrix, which is the case if the Eq. (4) is fulfilled and then the Mueller matrix is termed Mueller-Jones matrix [28]:

$$Tr(M^T M) = 4m_{00}^2 \quad (4)$$

Where Tr denotes the trace and T the matrix transpose operation. If the values of Eq. (4) are within $0 \leq Tr(M^T M)/4m_{00}^2 < 1$, it means the system depolarizes and, as a consequence, it can not be described by a Jones matrix. As a matter of fact, a Jones matrix can still depolarize light that is partially polarized [29].

Other useful auxiliary polarimetric parameters are the diattenuation, $D(M)$, and the polarizance parameters, $P(M)$, which are defined as [30]

$$0 \leq D(M) = \sqrt{m_{01}^2 + m_{02}^2 + m_{03}^2}/m_{00} \leq 1 \quad (5a)$$

$$0 \leq P(M) = \sqrt{m_{10}^2 + m_{20}^2 + m_{30}^2}/m_{00} \leq 1 \quad (5b)$$

$D(M)$ describes the diattenuation associated to a given system and indicates the intensity variation when an incident polarized state is transmitted or reflected. The upper limit, 1, is associated to a totally diattenuating system, while the lower value, 0, means the system does not attenuate at all. $P(M)$ is interpreted as the capability of a given system to polarize unpolarized incident light; a high value is associated to a highly efficient polarizer, but a lower value is associated to a low or null polarizer behavior. For example, an ideal linear polarizer is associated to a 1.0 value for both diattenuation and polarizance parameters, independently of the relative azimuthal orientation of its transmission axis with respect to the incident beam of light [31]. A system with intermediate values within the interval (0,1) is interpreted as a partial diattenuator or polarizer, respectively.

3. Experimental results and discussion

Employing a HeNe laser (632.8 nm), a polarization state generator (PSG), and a polarization state analyzer (PSA), a collimated beam with 2 mm wide was generated and sent toward the cylinder at normal incidence. As a way to show the simplicity of the system, an electric guitar string was employed as the metallic cylinder, placed at the center of an automated rotation stage of an angle-resolved scattering system (ARS), see Fig. 1a). The cylinder is a commercially available electric guitar nickel string, with a 254 μm diameter (Fender, 3150R Pure Nickel String, 0.01 inch diameter). The nickel has a refractive index of $1.98 + i3.74$ [32] and a skin depth of 0.013 μm to 0.633 μm wavelength, which ensures the light is not transmitted through the cylinder. The polarization state

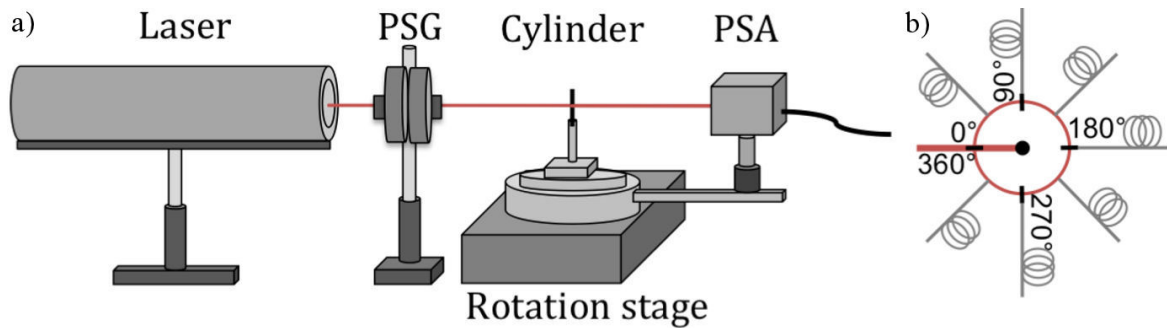


FIGURE 1. a) Experimental setup employed for the measurement of the light scattered by the metallic cylinder. b) A possible application as an optical fiber de-multiplexer.

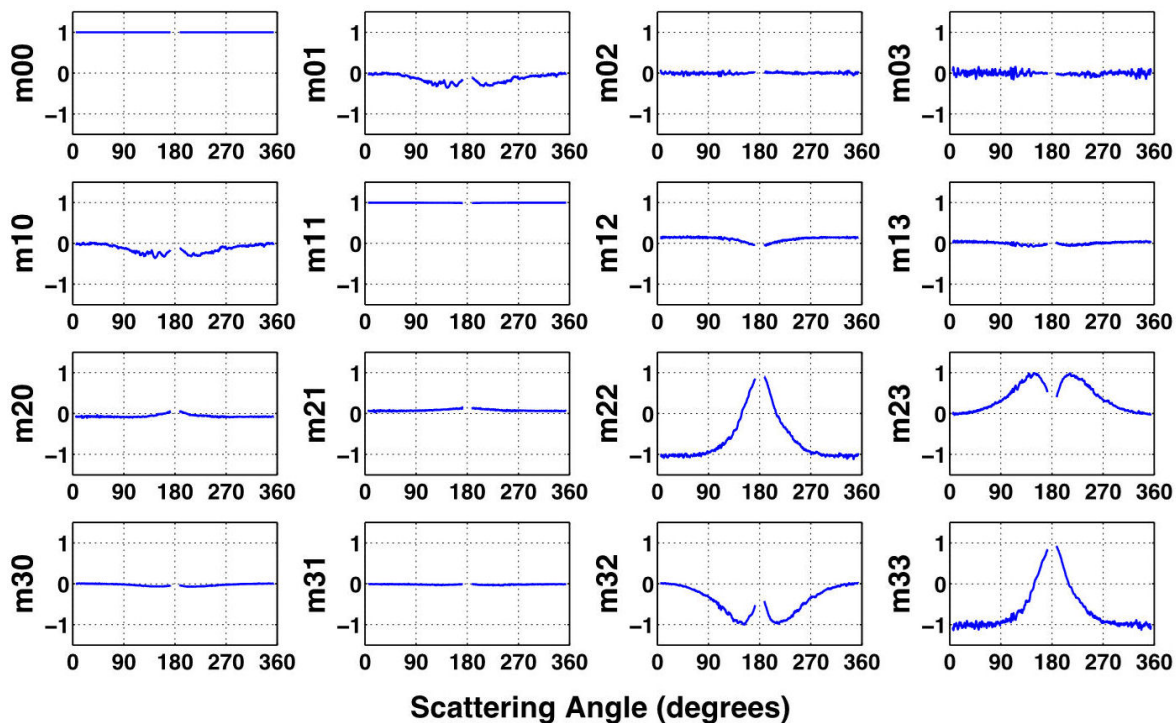


FIGURE 2. Normalized Mueller matrix parameters versus the scattering angle ($0^\circ < \theta_{\text{scatt}} < 360^\circ$), associated to the scattering of light by a metallic cylinder. Observe $m_{00} \cong m_{11}$, $m_{01} \cong m_{10}$, $m_{22} \cong m_{33}$, $m_{23} \cong -m_{32}$.

generator (PSG) consists of a linear polarizer of the Glan-Thompson type (Thorlabs, GTH10M), followed by a liquid crystal variable retarder with controller (Thorlabs, LCC1111-A and LCC25, respectively), both mounted in motorized rotation stages (Thorlabs, PRM1Z8E). The polarization state analyzer (PSA) is a commercially available head (Thorlabs, model PAX5710/VIS), which is mounted on a 40-cm-long arm and pointed toward the illuminated spot at the center of the cylinder. The experimental error of the complete system, including the laser fluctuations, is of the order of a 4%.

The scattered light is distributed on a plane surface, perpendicular to the cylinder axis. To obtain the Mueller matrix, a set of six polarization states was employed (linear horizontal, perpendicular, to $+45^\circ$, -45° , and circular right- and left-handed polarization states, respectively). In the absence of any polarization-sensitive effect in the optical medium placed

between the PSG and the PSA, the experimental setup was verified in order that each state of polarization detected corresponds to the same state of polarization generated.

The 36 intensities angularly-resolved measurements were handled by applying an algebraic algorithm to the data obtained [33], in order to get the 16 Mueller matrix parameters, which were plotted versus the scattering angle ($0^\circ < \theta_{\text{scatt}} < 360^\circ$). The Mueller matrix parameters are shown in Fig. 2, where the data around the direction of propagation, $\theta_{\text{scatt}} = 180^\circ$, have been omitted due to saturation present on the detector (we have not used stops or neutral spatial filters to cancel or attenuate the beam in that direction). In Fig. 2, the angularly-resolved Mueller matrix elements show that $m_{00} \cong m_{11}$, $m_{01} \cong m_{10}$, $m_{22} \cong m_{33}$, $m_{23} \cong -m_{32}$, and the elements m_{02} , m_{03} , m_{12} , m_{13} , m_{20} , m_{21} , m_{30} , m_{31} are almost zero. They are not exactly zero, probably due to

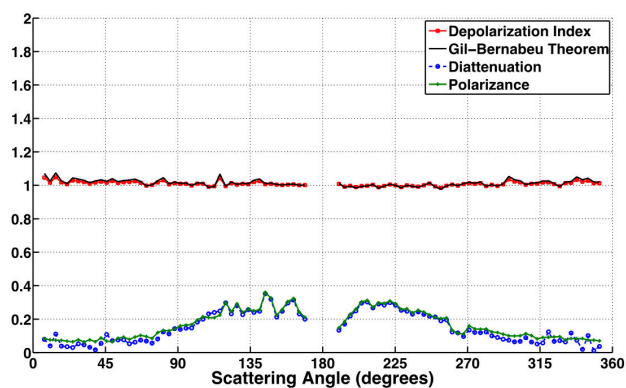


FIGURE 3. Polarization scalar metrics versus the scattering angle. Depolarization index (—■—), the Gil-Bernabeu theorem (—), the diattenuation (—○—) and the polarizance (—+—) parameters, respectively.

the fact that the commercial guitar string has some surface defects that scatters the light slightly. If we neglect the matrix elements that should be zero-valued, as expected from the discussed model, Eq. (2), we can conclude that the measured Mueller matrix of Fig. 2 confirms the model, Eq. (2). This is not an obvious result because a one-dimensional rough surface with any arbitrary profile is not a single cylinder.

Employing the MM values obtained from Fig. 2, some polarimetric parameters have also been computed. The Fig. 3 shows the depolarization index, Eq. (3), the Gil-Bernabeu theorem, Eq. (4), the diattenuation, Eq. (5a), and the polarizance parameters, Eq. (5b), respectively. All of them plotted in terms of the scattering angle (degrees).

The depolarization index, (—■—), takes on values around 1, with small oscillations, according to the resolution of the experimental setup employed here. The plot of the Gil-Bernabeu theorem, (—), shows the same behavior than the depolarization index; also observe the MM of Fig. 2 satisfies Eq. (4), the necessary and sufficient condition for a MM to be a Mueller-Jones matrix (represented as the ratio of the left-hand side divided by the right-hand side of Eq. (4)). At this stage, it is important to point out that a fully polarized incident beam is being used. It is well known that a 1D surface depolarizes light when multiple scattering effects are being present (under normal incidence), which is the case if the totally polarized incident light is scattered around 180° for a perfectly reflecting surface [9] or around 360° for a reflecting and transmitting surface. The results obtained here by applying the depolarization index or the Gil-Bernabeu theorem, prove there are not depolarization effects or if they are present, their contributions are within our experimental error complete system. In addition, by taking into account that each Mueller parameter m_{ij} is originated from the sum of four different and independent intensity measurements, probably the variation from the unity value for the depolarization index and the Gil-Bernabeu theorem, are originated by statistical speckle noise presented during the scattering process.

Other error factor can be due to the possible multiple reflections from the internal walls inside the head before reaching the detector (diameter size of 3 mm).

On the other hand, the diattenuation, Eq. (5a) and the polarizance parameters, Eq. (5b), have almost the same, slowly varying and symmetric behavior, with average maximum values of 0.25 around $80^\circ < \theta_{\text{scatt}} < 180^\circ$ and $180^\circ < \theta_{\text{scatt}} < 280^\circ$ and with average minimum values of 0.08 around $0^\circ < \theta_{\text{scatt}} < 80^\circ$ and $280^\circ < \theta_{\text{scatt}} < 360^\circ$. This means that the metallic cylinder can polarize un-polarized incident light, with an efficiency that depends on the scattering angle. Considering that $m_{01} = m_{10}$, $m_{20} = m_{30} = m_{02} = m_{03} = 0$, Eqs. (5) can be reduced approximately to a same angular behavior, $D(M) = m_{01}/m_{00} \cong m_{10}/m_{00} = P(M)$.

4. Conclusions

In summary, the experimental determination of the Mueller matrix associated to the light scattered from a metallic cylinder has been presented herein. Results show this Mueller matrix has the same form as those reported for the one-dimensional rough surfaces. A very important difference between a one-dimensional rough surface that scatters light around a complete circle and a metallic cylinder, is that the rough surface depolarizes angularly while the metallic cylinder does not. With the determination of the MM, useful information about polarimetric properties of the metallic cylinder can be obtained. The depolarization index and the Gil-Bernabeu theorem have shown that the light scattered by the metallic cylinder is not depolarized, within the experimental error of the system employed here, and therefore it could be described by the Jones formalism. As a consequence of the angular dependence of the scattering, the metallic cylinder surface can be tailored properly to handle the distribution of light and its polarization properties. Several useful devices could be constructed based in this easily controllable and accessible low-cost method. For example, one possible application of the scattering behavior by a metallic circular cylinder is to use it as a polarization-maintaining de-multiplexer in combination with the plastic optical fibers (POF). The POFs are easy to handle, flexible, and economical, so the applications with POFs have been developed and commercialized, from their use as a simple light transmission guide to their utilization as sensors [34]. The scattered light by the metallic cylinder can be distributed through the optical fibers, maintaining the same polarization of incident light in each output channels for the cases of parallel and perpendicular polarizations, respectively. For a general incident polarization state, the knowledge of the Mueller matrix allows to handle properly the desired polarization state, depending on the angular scattering position at which each single fiber is fixed (see Fig. 1b)). For instance, considering a circle with 12 cm radius (ignoring the sections on the circle where the incidence and the saturation are angularly located), it is possible to place up 30 output channels, separated 2 cm one of the other.

To our knowledge, this is the cheapest and easiest controllable way to generate linear horizontal and vertical polarizations scattered fully angularly and uniformly.

Acknowledgments

G.L.M. and I.S.O. acknowledge to the Becas Mixtas program (CONACYT-México) for the scholarships received to

spend their predoctoral leave at the University of Dayton (UD). R.E.L. also acknowledges to CONACYT (project No. 232956) for the financial support to spend his Sabbatical Year at UD.

-
1. M. Nieto-Vesperinas and J.M. Soto-Crespo, *Opt. Lett.* **12** (1987) 979.
 2. M.-J. Kim, J.C. Dainty, A.T. Friberg, and A.J. Sant, *J. Opt. Soc. Am. A* **7** (1990) 569.
 3. E.R. Méndez, M.A. Ponce, V. Ruiz-Cortés, and Z.-H. Gu, *Appl. Opt.* **30** (1991) 4103.
 4. Y. Kuga, C.T.C. Ce, A. Ishimaru, and L. Ailes-Sengers, *IEEE Transactions on Geoscience and Remote Sensing* **34** (1996) 1300.
 5. F.J. García-Vidal and L. Martín-Moreno, *Phys. Rev. B* **66** (2002) 155412.
 6. K.A. O'Donnell and M.E. Knotts, *J. Opt. Soc. Am. A* **8** (1991) 1126.
 7. N.C. Bruce, A.J. Sant, and J.C. Dainty, *Opt. Commun.* **88** (1992) 471.
 8. T.R. Michel, M.E. Knotts, and K.A. O'Donnell, *J. Opt. Soc. Am. A* **9** (1992) 585.
 9. M.E. Knotts, T.R. Michel, and K.A. O'Donnell, *J. Opt. Soc. Am. A* **10** (1993) 928.
 10. G. Atondo-Rubio, R. Espinosa-Luna, and A. Mendoza-Suárez, *Opt. Commun.* **244** (2005) 7.
 11. D.H. Goldstein, *Polarized Light* (CRC Press, New York, 2011).
 12. S.N. Savenkov, p. 1175, Ch. 29, in *Handbook of Coherent-Domain Optical Methods*, V.V. Tuchin, ed. (Springer, NY, 2013).
 13. F. Kuik, J.F. de Haan, and J.W. Hovenier, *Appl. Opt.* **33** (1994) 4906.
 14. D. Felbacq, G. Tayeb, and D. Maystre, *J. Opt. Soc. Am. A* **11** (1994) 2526.
 15. G. Sonnichsen, T. Franzl, T. Wilk, G. von Plessen, and J. Feldmann, *Phys. Rev. Lett.* **88** (2002) 077402.
 16. A. Kienle, F.K. Forster, and R. Hibst, *Opt. Lett.* **29** (2004) 2617.
 17. C.J. Murphy, A.M. Gole, S.E. Hunyadi, and C.J. Orendorff, *Inorganic Chem.* **45** (2006) 7544.
 18. S.-C. Lee, *J. Opt. Soc. Am. A* **28** (2011) 1067.
 19. F. Frezza, L. Pajewski, C. Ponti, G. Schettini, and N. Tedeschi, *IEEE Geosc. Rem. Sens. Lett.* **10** (2013) 179.
 20. H.C. Van der Hulst, *Light Scattering by Small Particles* (Dover, Amsterdam, 1957).
 21. L.M. Sanchez-Brea, P. Siegmann, M.A. Rebollo, and E. Bernabeu, *Appl. Opt.* **39** (2000) 539.
 22. E. Bernabeu, I. Serroukh, and L.M. Sanchez-Brea, *Opt. Eng.* **38** (1999) 1319.
 23. G. Videen and W.S. Bickle, *Appl. Opt.* **31** (1992) 3488.
 24. G. Videen and D. Ngo, *J. Opt. Soc. Am. A* **14** (1997) 70.
 25. I. Saucedo-Orozco, G. López-Morales, and R. Espinosa-Luna, *Opt. Lett.* **39** (2014) 5341.
 26. C.F. Bohren and D.R. Huffman, *Absorption of Light by Small Particles* (New York, 1983).
 27. J.J. Gil and E. Bernabeu, *Opt. Acta* **33** (1986) 185.
 28. J.J. Gil and E. Bernabeu, *Opt. Acta* **32** (1985) 259.
 29. C. Brosseau, *Opt. Commun.* **131** (1996) 229.
 30. S.Y. Lu and R.A. Chipman, *Opt. Commun.* **146** (1998) 11.
 31. R. Espinosa-Luna, G. Atondo-Rubio, E. Bernabeu, and S. Hinojosa-Ruíz, *Optik* **121** (2010) 1058.
 32. E.D. Palik, *Handbook of Optical Constants of Solids* (Academic, New York, 1985). p. 323.
 33. K.M. Salas-Alcántara, R. Espinosa-Luna, I. Torres-Gómez and Y.O. Barmenkov, *Appl. Opt.* **53** (2014) 269.
 34. J. Zubia and J. Arrue, *Opt. Fiber Technol.* **7** (2001) 101.